VOL. 11, NO. 4, FEBRUARY 2016 ISSN 1819-6608
ARPN Journal of Engineering and Applied Sciences

www.arpnjournals.com

THERMAL RESPONSE OF CONVECTIVE BOUNDARY LAYER STAGNATION FLOW OF NANOFLUID OVER SHRINKING SURFACE INFLUENCING SUCTION AND VARIABLE STREAM CONDITIONS

Vibhu Vignesh Balachandar[1], Sulaiman Bin Hasan[1], Ashwin kumar[1] and R. Kandasamy[2]
[1]Faculty of Mechanical and Manufacturing Engineering, Parit Raja, Batu Pahat, Johor, Malaysia
[2]Faculty of Science, Technology and Human Development, Universiti Tun Hussein Onn Malaysia, Parit Raja, Batu Pahat, Johor, Malaysia
E-Mail: vibhuvignesh3@gmail.com

ABSTRACT

In this paper, we analysed convective boundary layer stagnation point flow of nanofluid influencing by suction and magnetic field over a porous shrinking surface is investigated numerically and simulated with Maple 18 Software. Thermophoresis and Brownian motion effects are included in the nanofluid model. Governing nonlinear boundary layer equations for momentum, energy and continuity equations are transformed into a system of nonlinear ordinary coupled differential equations by using similarity transformations. The effects of physical parameters on nanofluid (Liquid and Gaseous) are analysed. It is found that for a certain range of injection process, solutions exists for velocity flow, temperature flow and volume concentration. It tends to provide solutions for skin friction, rate of heat and rate of mass transfer of nanofluids (Liquid and Gaseous).

Keywords: stagnation point flow, nanofluid, brownian motion, thermophoresis, magnetic field.

INTRODUCTION

Heat transfer is one of the top technical challenges faced by high-tech industries such as manufacturing, metrology, microelectronics, nuclear reactors, domestic refrigerator, grinding, machining, ships, hybrid-powered engines, chillers, space technology, boiler flue gas temperature reduction, vehicle thermal management and defense. These industries facing heat transfer problems because of unprecedented heat loads and heat fluxes. To overcome the heat transfer issue, nanofluids are termed.

Nanofluids attains more attention from researchers due to its enhanced properties. This innovative fluid for heat transfer was introduced (Choi, 1995). Suspending nanoparticles into base fluids attains unique physical properties as well as chemical properties increases the thermal conductivity and therefore substantially nanofluid enhances the heat transfer characteristics. Nanofluid consisting of metallic and non-metalic solid nanoparticles with sizes typically on the order of 1–100 nm, dispersing evenly in a base fluid such as air, liquid, toluene and liquid nitrogen (Wang, 2008).

The boundary layer flow of nanofluid influencing by magnetic field has numerous applications in engineering problems such as MHD generator, power generation in nuclear reactors, petroleum industries, power plants and Coal extraction. Considering the quality of operation process, radiative heat transfer in the boundary layer plays vital role in applications. Quality of process depends on the ambient fluid particles heat transfer rate. Usually nanofluid includes the effects of thermophoresis and Brownian motion (Buongiorno, 2006). He stated that nanofluids flow have affected by many physical factors given (Kuznetsov, 2010), (Nield, 2009), but Brownian motion and thermophoresis plays vital role.

The steady flow over a porous surface is a major experimental research all over the industries in past recent years due to its numerous application behind in it. On another hand stagnation point flow over stretching/ shrinking sheet studies also going on with many application oriented process. Nanofluid subjected to stagnation point flow possesses highest pressure, highest heat transfer and the highest rate of mass decomposition. (Miklavcic and Wang, 2006) investigated stagnation point flow and obtained duel solution. He also obtained steady viscous flow in the investigation of boundary layer flow near a shrinking surface. Mass transfer through shrinking sheet was investigated (Fang *et al.* 2009). Unsteady three dimensional boundary layer flow due to a permeable shrinking sheet was analysed (Bachok *et al.* 2010).

Hamad and Ferdows (2011), investigated the boundary layer flow of electrically conducting fluid and heat transfer over a shrinking surface. They studied different types of nanoparticles and found each nanoparticle differs from others in physical characteristics each possess different character. They enclosed that changing the nanoparticle type changes the behaviour of the fluid flow. Numerous studies on nanofluids are undergoing (Bachok *et al.* 2011, 2012), (Mankinde, 2011), Alsaedi *et al.* 2012), (Ibrahim *et al.* 2013). Magyari and Keller (1999), have obtained the similarity solutions which describe the steady plane boundary layers on a shrinkinging sheet with flow of temperature distribution analytically. The numerical solution was obtained (Al-odat *et al.* 2006) for thermal boundary layer on shrinking sheet with temperature distribution due to the effect of magnetic field. Following them many researchers (Biliana, 2009), (Ishak, 2011), (Bala, 2011) investigated the numerical solutions for the boundary layer flow problem over shrinking sheet. kameswaran *et al.* (2012), derived an analytical solution for Newtonian liquid flow on

exponential shrinking sheet due to radiation effects and observed that the species boundary layer thickening with the increase in increase of magnetic parameter.

The present paper is to study the simultaneous effect of the thermal radiation and magnetic field on the heat transfer and fluid flow of boundary layer flow on porous surface. Results presented focus on how the magnetic field, porosity, Brownian motion, thermophoresis and thermal radiation affects the nanofluid characteristics.

FLOW ANALYSIS

Consider the steady two-dimensional MHD stagnation-point flow of an incompressible viscous electrically conducting nanofluid impinging normally on porous shrinking surface. The fluid is subjected to a uniform transverse magnetic field of strength B_0. Figure. 1 describes the coordinate system and physical model. The axis x measured along the porous medium surface and axis y normal to it.

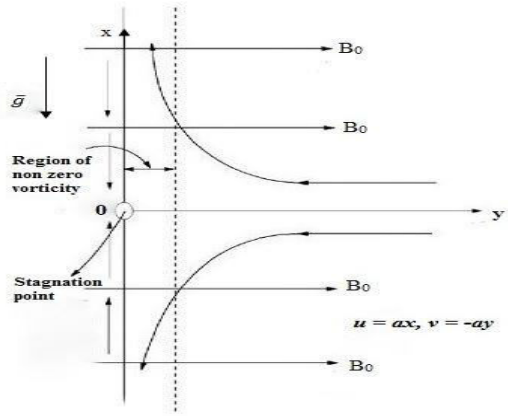

Figure-1. Physical model and the coordinate system.

It is assumed that the velocity of the porous shrinking surface is $u_w(x) = cx$ and the velocity outside boundary layer is $U(x) = ax$, where a and c are constants with $a > 0$. We note that $c < 0$ correspond to porous shrinking surface, $\bar{g}$ corresponds to gravitational forces. Cartesian coordinates x and y of the energy, momentum and continuity equations for nanofluids can be written as (Lok *et al.* 2011).

$$\frac{\partial u}{\partial x} + \frac{\partial v}{\partial y} = 0 \tag{1}$$

$$u\frac{\partial u}{\partial x} + v\frac{\partial u}{\partial y} = U\frac{dU}{dx} + v\frac{\partial^2 u}{\partial y^2} + \left(\frac{\sigma B_0^2}{\rho_f} + \frac{v}{k}\right)(U-u) + g\beta(T - T_\infty) + g\beta^*(C - C_\infty) \tag{2}$$

$$u\frac{\partial T}{\partial x} + v\frac{\partial T}{\partial y} = \alpha_m\frac{\partial^2 T}{\partial y^2} - \frac{1}{\rho_f c_p}\frac{\partial q_r}{\partial y} + \tau\left[D_B\frac{\partial c}{\partial y}\frac{\partial T}{\partial y} + \frac{D_T}{T_\infty}\left(\frac{\partial T}{\partial y}\right)^2\right] \tag{3}$$

$$u\frac{\partial C}{\partial x} + v\frac{\partial C}{\partial y} = D_B\frac{\partial^2 C}{\partial y^2} + \frac{D_T}{T_\infty}\frac{\partial^2 T}{\partial y^2} \tag{4}$$

We have analysing the flow with influencing magnetic field, so we have induced magnetic field in Equation. (2). This assumption is justified for flow of electrically conducting fluids such as liquid metals e.g., mercury, liquid sodium etc. Let the velocity components along the x and y axes are u and v, free stream velocity ($U(x)$), porous medium permeability (k), specific heat at constant pressure (c_p), radiative heat flux (q_r), nanoparticle volume fraction (C), Brownian diffusion coefficient (D_B), electrical conductivity of the fluid (σ), kinematic viscosity (v), thermal diffusivity (α_m), base fluid density (ρ_f), thermophoresis diffusion coefficient (D_T) and ratio of the effective heat capacity of the nanoparticle material to the heat capacity of the ordinary fluid (τ), fluid temperature (T). The nanoparticle volume fraction (C_w) and the wall temperature (T_w) are assumed to be constant at the surface and also when y tends to infinity, the ambient values of the nanoparticle volume fraction C_∞ and the temperature T_∞ attain to be constant values respectively. The boundary conditions of shrinking surface:

$$v = v_0, u = u_w(x) = cx, C = C_w, T = T_w \text{ at } y = 0;\quad T \to T_\infty, u \to U(x) = ax, C \to C_\infty \text{ as } y \to \infty \tag{5}$$

By Rosseland approximation, (Bachok *et al.*, 2012) the radiative heat transfer as

$$q_r = -\frac{4\delta}{3k_1}\frac{\partial T^4}{\partial y} \tag{6}$$

Where, mean absorption coefficient (k_1) and Stefan–Boltzmann constant (δ). Assuming within the flow the temperature difference is such that T^4 in Taylor series it can be expanded about T_∞ and neglecting higher order terms, we get $T^4 \approx 4T_\infty^3 T - 3T_\infty^4$. Hence Equation. (7) becomes,

$$\frac{\partial q_r}{\partial y} = -\frac{16\delta T_\infty^3}{3k_1}\frac{\partial^2 T}{\partial y^2} \tag{7}$$

The dimensionless variables and the stream function can be defined as follows:

$$\psi = \sqrt{av}\,x f(\eta)\ ;\quad \varphi(\eta) = \frac{C - C_\infty}{C_w - C_\infty}\ ;\quad \theta(\eta) = \frac{T - T_\infty}{T_w - T_\infty}\ ;\quad \eta = y\sqrt{\frac{a}{y}} \tag{8}$$

Where, $(\psi)$the stream function defined as $v = -\frac{\partial\psi}{\partial x}$ and $u = \frac{\partial\psi}{\partial y}$. Based on the above mentioned stream functions, Equations. (1) - (4) become

$$f''' + ff'' - f'^2 + (M + \lambda)(1 - f') + Gr\theta + Gm\varphi + 1 = 0 \tag{9}$$

$$\frac{1}{Pr}\left(1 + \frac{4R}{3}\right)\theta'' + f\theta' + N_b\theta'\varphi' + N_t\theta'^2 = 0 \tag{10}$$

VOL. 11, NO. 4, FEBRUARY 2016 ISSN 1819-6608
ARPN Journal of Engineering and Applied Sciences

www.arpnjournals.com

$$\varphi'' + Le\, f\, \varphi' + \frac{N_t}{N_b}\theta'' = 0 \tag{11}$$

Where $M = \frac{\sigma B_0^2}{\rho_f a}$- magnetic parameter, $R = \frac{4\delta T_\infty^3}{3k_1\alpha_m}$- thermal radiation parameter, $Pr = \frac{v}{\alpha_m}$- Prandtl number, $Gr = \frac{g\beta(T_w - T_\infty)}{aU}$- Grashof number and $Gm = \frac{g\beta^*(C_w - C_\infty)}{aU}$-modified Grashof number, $N_b = \tau\frac{D_B(C_w - C_\infty)}{v}$- Brownian motion parameter, $\lambda = \frac{v}{ak}$-porous parameter, $N_t = \frac{\tau D_T(T_w - T_\infty)}{vT_\infty}$- thermophoresis parameter, $S = \frac{v_0}{\sqrt{av}}$- suction parameter, $Le = \frac{v}{D_B}$- Lewis number. The temperature really does not depend on (Pr) and (R) independently is presented at Equation. (10), but depend on a combination, $Pr_{eff} = \frac{Pr}{(1+4\frac{R}{3})}$. which is the effective Prandtl number. Equation. (10) can be written as

$$\frac{1}{Pr_{eff}}\theta'' + f\theta' + N_b\theta'\varphi' + N_t\theta'^2 = 0 \tag{12}$$

with boundary conditions:

$$\theta(0) = 1, \varphi(0) = 1, f(0) = S, f'(0) = \alpha = \frac{c}{a}, f'(\infty) = 1, \theta(\infty) = 0, \varphi(\infty) = 0$$

Where, the ratio of rates of the shrinking velocity and the free stream velocity is α.

RESULT AND DISCUSSION

The set of equations (9), (10) and (11) is highly nonlinear. It can be solve analytically and numerically by manual, subject to the boundary conditions (13) but it is not easy and it take month of time to get numerical solutions. So in this research we use MAPLE 18 the very robust computational algebra software to get the analytical and numerical solutions. Fourth-fifth order Runge–Kutta–Fehlberg method is used by this software as default to solve boundary value problems numerically. The transformed system represented in the form of the governing equations momentum, energy and continuity by coupled nonlinear ordinary differential equations (9), (10) and (11) with boundary conditions (13). Computations are carried out for several sets of values of the streaming condition parameters, namely, Lewis number (Le), thermal radiation parameter (R), Brownian motion parameter (N_b), magnetic parameter (M), effective Prandtl number (Pr_{eff}), thermophoresis parameter (N_t), shrinking sheet ($\alpha < 0$), and suction $S > 0$. In order to serve the salient features of the model, the numerical results are presented in the following figures with fixed parameters,

$M = 1, N_t = 0.05, N_b = 0.01, R = 0.2, Le = 1.0, \lambda = 0.3, Gr = 3, Gm = 3, S = 1,$

and shrinking parameter $\alpha = -1.20$.

In order to validate our results, In Table 1 we compared the results of (Lok *et al.* 2014) and (Hamad., & Wang, 2008) with our present results of $\boldsymbol{f''(0)}$. The present results shows a good agreement with (Lok *et al.* 2014) and (Hamad., & Wang, 2008) results since the errors are found to be very minimum.

Table-1. Comparison of the present results for with published works.

M	$\alpha = \frac{c}{a}$	Lok *et al.* (2014)	Wang (2008)	Present results
0	0.0	1.232588	1.232588	1.232587542
	0.1	1.146561	1.146560	1.146560893
	0.2	1.051130	1.051130	1.051130448
	0.5	0.713295	0.713300	0.713298653
	1.0	0.000000	0.000000	0.000000001
	5.0	-10.264749	-10.26475	-10.26474869

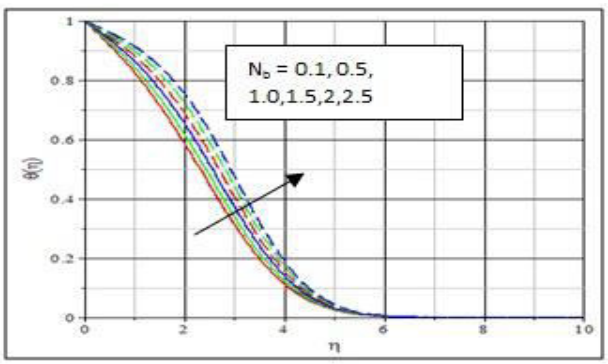

(a)

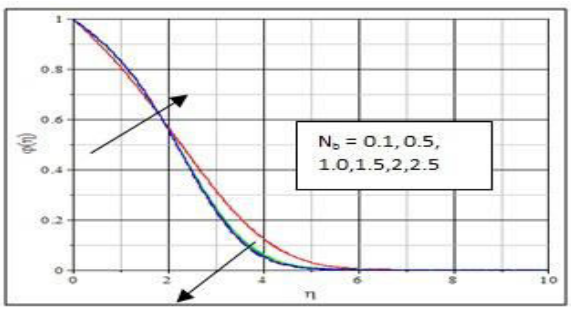

(b)

Figure 2. (a)-2(b): Brownian motion on $\theta(\eta)$and$\varphi(\eta)$-comparison with Samir Kumar Nandy and Pop (2014).

Figures-2(a) – 2(b) depicts the precision with the theoretical solution of θ(η)and φ(η) profiles for different

values of Brownian motion (N_b) exactly correlates with the first solution of Samir Kumar Nandy and Pop [9].

The effect of porosity and magnetic strength on velocity distribution of two different nanofluids on shrinking porous sheet with suction pressure are shown in Figure-3 and Figure-4. In Figure-3 it shown that increasing of kinematic viscosity and decreasing of porous surface permiability, the velocity of nanofluids increases with increase of porosity. From Figure-4 it observed that the velocity of nanofluids increase with increase of magnetic effect. The lorentz force usually acts in opposite direction against the nanofluid flow, opposing the motion of the nanofluid but suction provides an additional effect to the nanofluid flow. It makes the fluid to move at a retarded rate. It is interesting to note that the momentum boundary layer for M is equal to the momentum boundary layer of λ . It is because of the combined effect of Brownian motion and thermophoresis nanoparticle deposition on shrinking surface. There is liquid / gaseous nanofluid momentum $\eta = 0.75$ / $\eta = 0.95$ for λ and M. Comparing the nanofluids, gaseous nanofluid has higher velocity than the liquid nanofluid. It is because of fluid viscosity and friction on porous surface. From Table-2 we can understand the rate of skin friction of liquid and gaseous nanofluids. The rate of skin friction is higher in liquid nanofluids during porosity effect as well as Magnetic effect. this is due to the viscosity of liquid nanofluids.

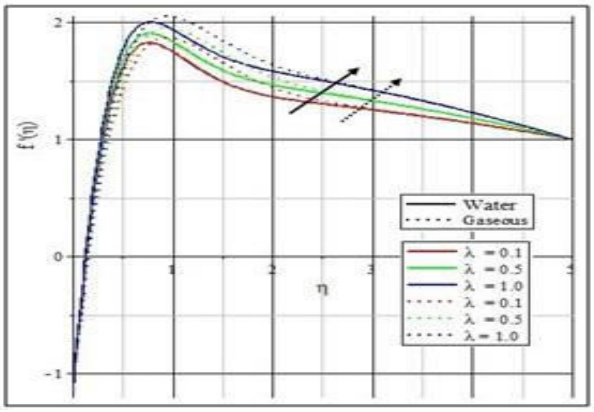

Figure-3. Porosity effects on velocity profiles.

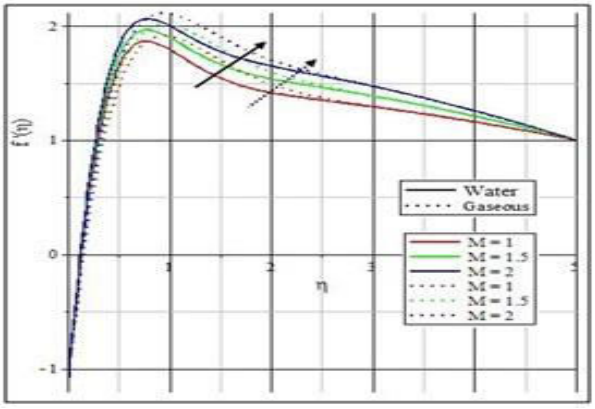

Figure-4. Magnetic effects on velocity profiles.

Table-2. Comparison of skin friction between liquid and gaseous nanofluids subjected to porosity and Magnetic field.

	Brownian motion Parameter (N_b)	Liquid Nanofluid	Gaseous nanofluid
Skin friction (f'') of Porosity parameter	0.1	9.937432793931299	8.63381325786874
	0.5	10.212744835391169	8.930883770065766
	1.0	10.551311709898943	9.29503333474292
Skin friction (f'') of Magnetic parameter	1.0	10.075603365176612	8.783010885027801
	1.5	10.416600447183708	9.150297560984571
	2.0	10.751661795609998	9.50992033067232

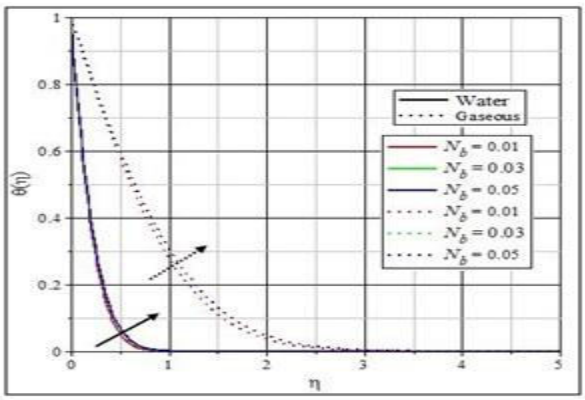

Figure-5. Brownian motion on temperature distribution.

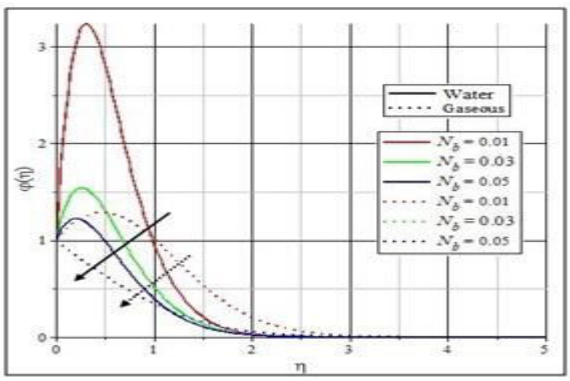

Figure-6. Brownian motion on nanoparticle volume fraction.

Figures-5 and 6 presents the variation in temperature and nanoparticle volume concentration profiles of two different nanofluids subjected to Brownian motion with the influence of suction and magnetic effect. Figure-5 shows that, increase in Brownian motion parameter increases thermal boundary layer and decreases nanoparticle volume concentration for both gaseous and liquid nanofluids respectively. The physics behind this is, increased Brownian motion increases the thermal boundary layer thickness and then decreases the diffusion boundary layer thickness, which ultimately decelerates nanoparticle volume fraction and enhances the temperature. It is noted that on nanoparticle volume fraction, strength of the magnetic field plays an important factor, Figure-2(b) $M \neq 0$ and Figure-5 $M = 1$ whereas there is no significant change in temperature profile, as well as Figure-2(a) $M = 0$ and Figure-6 $M = 1$. Thermal and diffusion behaviours of nanoparticles at nanoscale level are governed by various parameters. It is noted that Brownian motion on nanoparticles plays a vital role in governing these behaviour of nanoparticles. Due to the size of particles in nanofluids system Brownian motion occurs, which could affect heat transfer properties. As the size of the particle reaches to the nano-meter scale, the Brownian motion of the particles and its effects on the neighbouring liquids play a vital role in heat transfer. This is because the Brownian motion enhances thermal conduction due either to nanoparticles transporting heat or the micro convection of the fluid surrounding individual nanoparticles. From Table-3 we can understand the rate of heat and mass transfer of liquid and gaseous nanofluids. As subjected to Brownian motion both the rate of heat transfer and mass transfer is higher in Gaseous nanofluids than the liquid nanofluids, it is because of suction pressure which liquid from high pressure area to low pressure area.

Table-3. Comparison of rate of heat and mass transfer between liquid and gaseous nanofluids subjected to Brownian motion.

	Brownian motion Parameter (N_b)	Liquid Nanofluid	Gaseous Nanofluid
Rate of heat transfer ($-\theta'$)	0.01	4.2375686340378795	0.9489617861729504
	0.03	4.167945110329799	0.7002846627316452
	0.05	4.21287171643839	0.9091818557851019
Rate of mass transfer ($-\varphi'$)	0.01	4.2375686340378795	1.312486469806002
	0.03	4.854689086639787	0.5699840785650471
	0.05	2.4779786424235644	0.7952045516188634

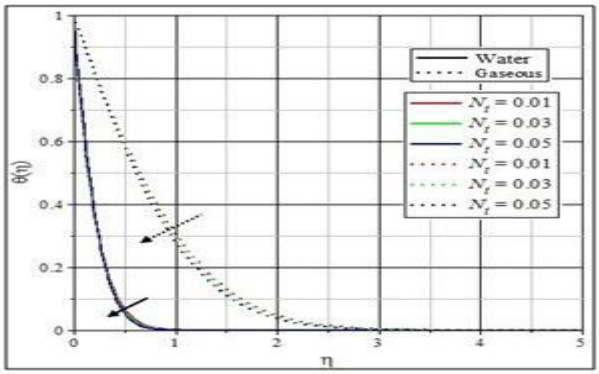

Figure-7. Thermophoresis on temperature distribution.

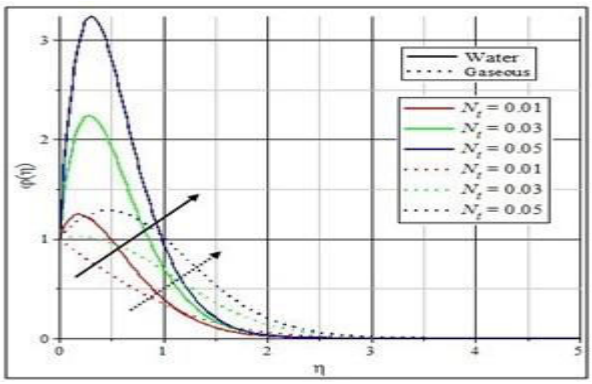

Figure-8. Thermophoresis on nanoparticle volume fraction.

Figures-7 and 8 depict the variation in temperature and nanoparticle volume concentration profiles of two different nanofluids subjected to thermophoresis with the influence of suction and magnetic effect. Figure-7 shows that, increase in thermophoresis parameter decreases thermal boundary layer and increases nanoparticle volume concentration for both liquid and gaseous nanofluids respectively. It is observed that the thermal boundary layer thickness of gaseous nanofluid is slightly decreased than liquid nanofluid.

While diffusion boundary layer strongly increases with increase in thermophoresis parameter (N_t) for both nanofluids. The thermophoresis states that the fact, increasing the temperature of nanoscale sized particle in base fluid will acquire momentum from heated surface and moves on. Gaseous nanofluid acquires momentum from heated surface and spreads throughout the boundary where

liquid nanofluid moves near the surface. We perceive that, negative N_t point out a hot surface and positive N_t to a cold surface. For hot surfaces, the nanoparticle volume fraction boundary layer is blow away from the surface by the high strength of thermophoresis, since a hot surface drives the Nano sized particles from it, thereby forming a relatively particle-free layer near the surface. On cold surface for higher values of thermophoretic parameter N_t that distinctive peaks in the profiles occur in region adjacent to the wall. This means that the nanoparticle volume fraction near the surface is higher than the nanoparticle volume fraction at the surface and consequently, due to the thermophoretic effect the nanoparticles are expected to transfer to the surface. As a result, the diffusion boundary layer is formed just outside. In particular, increasing the thermophoresis N_t, slightly increases thermal boundary layer but strongly increases the nanoparticle diffusion boundary layer. From Table-4 we can understand the rate of heat and mass transfer of liquid and gaseous nanofluids. As subjected to thermophoresis the rate of heat transfer and mass transfer is higher in Gaseous nanofluids than the liquid nanofluids, it is because of suction pressure which liquid from high pressure area to low pressure area.

Variation in temperature and nanoparticle volume concentration profiles of two different nanofluids in the presence of suction and magnetic effect is figured in Figures-9 and 10. According to equations (1.2) and (1.3), the divergence of the radiative heat flux decreases as thermal conductivity of the nanofluid raises which in turn decreases the rate of radiative heat transfer to the nanofluid and hence the nanofluid temperature accelerates whereas from Figure-10 the profile of nanoparticle volume fraction of on shrinking porous surface firstly decreases $(0 \le \eta \le 0.75)$ / $(0 \le \eta \le 1.5)$ and then increases $(\eta \ge 0.75)$ / $(\eta \ge 1.5)$.From here we observed that, the thermal radiation effect becomes more significant as $R \to 0 (R \neq 0)$ and when $R \to \infty$ it can be neglected. It is perceive that the nanofluid temperature enhances with increase of the thermal radiation parameter R. Porosity and absorption of shrinking surface induces combined effect on radiation parameter, tends to enhance the temperature significantly in flow region. The total amount of radiation of all frequencies increases steeply as the temperature rises and accelerates the nanoparticle volume fraction; it grows as T^4, where T is the absolute temperature of the nanoparticle. This is the fact that the thermal radiation is one of the principal mechanisms of heat transfer. The velocity of liquid and gaseous nanofluid increases as the radiation increases on shrinking surface. The Figure-9 depict temperature profile for gaseous nanofluid is more than the temperature profile of liquid nanofluid. This is due to the fact that thermal boundary layer thickness changes with change in the thermal radiation strength of nanofluid. From Table-5 we can understand the rate of heat and mass transfer of liquid and gaseous nanofluids. As subjected to thermal radiation the rate of heat transfer and mass transfer is higher in Gaseous nanofluids than the liquid nanofluids, it is because of suction pressure which liquid from high pressure area to low pressure area.

Table-4. Comparison of rate of heat and mass transfer between liquid and gaseous nanofluids subjected to therrmophoresis.

	Thermophoresis parameter (N_t)	Liquid Nanofluid	Gaseous nanofluid
Rate of heat transfer ($-\theta'$)	0.01	4.778253195415301	0.9097405311251388
	0.03	4.237568634093304	0.9311692318491236
	0.05	0.9097405311251388	0.9489617862484533
Rate of mass transfer ($-\varphi'$)	0.01	3.047956963444409	0.7946380545396571
	0.03	1.025512086783092	0.2510171650162266
	0.05	0.7946380545396571	1.3124864696352503

Table-5. Comparison of rate of heat and mass transfer between liquid and gaseous nanofluids subjected to thermal radiation.

	Thermal radiation parameter (R)	Liquid Nanofluid	Gaseous nanofluid
Rate of heat transfer ($-\theta'$)	0.1	4.569690668794884	1.0163125897182665
	0.5	3.5030187774102695	0.8037429349318448
	1.0	2.7647903903213407	0.6593781652418993
Rate of mass transfer ($-\varphi'$)	0.1	18.680636552773542	1.5932169713526734
	0.5	13.379930693251628	0.7269537068108507
	1.0	9.749920374255685	0.17781681226611165

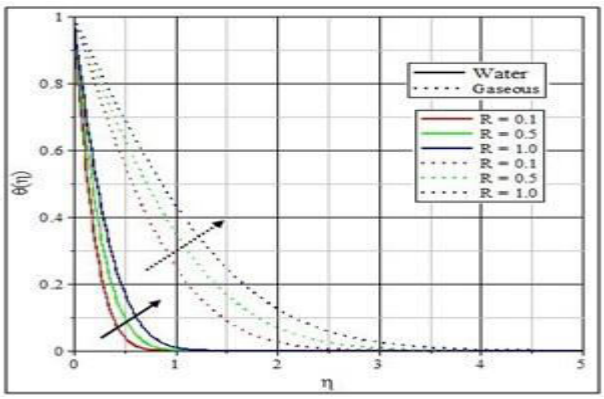

Figure-9. Thermal radiation on temperature distribution.

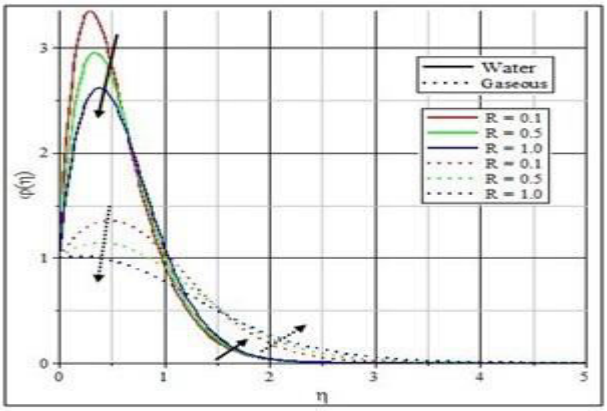

Figure-10. Thermal radiation on nanoparticle volume fraction.

CONCLUSIONS

Thermal response of convective boundary layer stagnation point flow of two nanofluids (liquid and gaseous) over porous shrinking surface influencing suction pressure with various stream condition parameters like magnetic, porosity, Brownian motion, thermophoresis, thermal radiation parameters on flow field velocity, heat transfer characteristics and nanoparticle volume concentration is investigated. The results obtained are in excellent agreement with the previously published data available in the literature in limiting condition for some particular cases of the present study. The effects of these parameters on the velocity distribution, temperature distribution and nanoparticle volume fraction can be summarized as follows:

- It is interesting that the momentum of the nanofluid increases with increase of the magnetic strength for both liquid and gas nanofluid over porous shrinking surfaccet. The lorentz force usually acts in opposite direction against the nanofluid flow, opposing the motion of the nanofluid but suction provides an additional effect to the nanofluid flow. Comparing the nanofluids, gaseous nanofluid has higher velocity than the liquid nanofluid. It is because of fluid viscosity and friction on porous surface.
- It is noticed that the Brownian and thermophoresis motion of the nanoparticles provides an alternative force in the flow region and its effect on surrounding liquids, plays a major role in heat and mass transfer characteristics whereas thermal and diffusion behaviours of nanoparticles at nanoscale level is governed by various parameters. It is noted that nanoparticles Brownian motion is important factor in governing these behaviour of nanoparticles. Due to size of nanoparticles Brownian motion takes place in nanofluids system which has a chance of affecting heat transfer properties..
- The effect of thermal radiation on nanofluids influenced by magnetic effect and suction pressure is to enhance the temperature. The temperature of the nanofluid enhances with increase of the thermal radiation parameter R. Porosity and absorption of shrinking surface induces combined effect on radiation parameter, tends to enhance the temperature significantly in flow region. Due to the effect of suction, shrinking surface exerts a force in flow region over diffusion boundary layer hence the nanofluid temperature accelerates whereas the nanoparticle volume fraction of liquid/ gaseous nanofluid on shrinking porous surface firstly decreases and then increases $(\eta \geq 0.75)$ / $(\eta \geq 1.5)$.
- As subjected to stream conditions the skin friction, rate of heat transfer and rate of mass transfer is higher in Gaseous nanofluids as compared to liquid nanofluids. It is because of suction pressure which liquid from high pressure area to low pressure area.

We may conclude the flow and heat transfer properties of convection boundary layer flow in the stagnation-point region influencing suction and magnetic field on nanoparticles in liquid and gaseous base fluid can be controlled by changing the quantity of the thermophoresis and Brownian motion. The problem of nanofluid flow and heat transfer at a stagnation-point region has important applications in many fields such as the power generation in nuclear reactors,nuclear reactor coolant, the aerodynamic of plastic sheet, the centralized cooling system of high grade machinaries, and so forth.

REFERENCES

[1] Al-Odat, M.Q., Damseh, R.A., Al-Azab, T.A. (2006). Thermal boundary layer on an exponentially stretching continuous surface in the presence of magnetic field effect. International Journaal of Applied Mechanical Engineering 11(2), pp. 289–99.

[2] Alsaedi, A., Awais, M., Hayat, T. (2012). Effects of heat generation/ absorption on stagnation-point flow of nanofluid over a surface with convective boundary conditions. Computational Nonlinear Science and Numerical Simulation 17, pp. 4210–4223.

[3] Bala, A.P., Bhaskar, R.N. (2011). Thermal radiation effects on hydro-magnetic flow due to an exponentially stretching sheet. International Journal of

Applied Mathematics and Computational dynamics 3(4) pp. 300–6.

[4] Bachok, N., Ishak, A., Pop, I. (2010). Boundary-layer flow of nanofluids over a moving surface in a flowing fluid. International Journal of Thermal Sciences 49(9), pp. 1663–1668.

[5] Bachok, N., Ishak, A., Pop, I. (2011). Stagnation-point flow over a stretching/shrinking sheet in a nanofluid. Nanoscale Research Letter 6, pp. 623–632.

[6] Bachok, N., Ishak, A., Pop, I., (2012). Flow and heat transfer characteristics on a moving plate in a nanofluid. International Journal of Heat and Mass Transfer 55, pp. 642–648.

[7] Buongiorno, J. (2006). Convective transport in nanofluids, ASME Journal of Heat Transfer 128, pp. 240–250.

[8] Bidin Biliana, Nazar Roslinda, (2009). Numerical solution of the boundary layer flow over an exponentially stretching sheet with thermal radiation. Europe Journal of Science and Research 33(4), pp. 710–7.

[9] Ishak, A. (2011) MHD boundary layer flow due to an exponentially stretching sheet with radiation effect. Sains Malaysiana 40(4) pp. 391–5.

[10] Choi, S.U.S. (1995). Enhancing thermal conductivity of fluids with nanoparticles. ASME Fluids Engineering Division 231, pp. 99–105.

[11] Fang, T., Zhang, J., Yao, S. (2009). Viscous flow over an unsteady shrinking sheet with mass transfer, China Physics Letter 26, pp. 014703.

[12] Hamad, M.A.A., Ferdows, M. (2011). Similarity solution of boundary layer stagnation-point flow towards a heated porous stretching sheet saturated with a nanofluid with heat absorption/ generation and injection/blowing: a lie group analysis. Computational Nonlinear Science and Numerical Simulation 17, pp. 132–140.

[13] Ibrahim, W., Sankar, B., Nandeppanavar, M.M. (2013). MHD stagnation point flow and heat transfer due to nanofluid towards a stretching sheet. International Journal of Heat and Mass Transfer 56, pp. 1–9.

[14] Kameswaran, P.K., Narayana, M., Sibanda, P., Makanda, G. (2012). On radiation effects on hydromagnetic Newtonian liquid flow due to an exponential stretching sheet. Boundary Value Problems 1(105) pp. 1–16.

[15] Kuznetsov, A.V., Nield, D.A. (2010). Natural convective boundary layer flow of a nanofluid past a vertical plate. International Journal of Thermal Science 49, pp. 243–247.

[16] Lok, Y.Y., Ishak, A., Pop, I. (2011). MHD stagnation-point flow towards a shrinking sheet, International Journal of Numerical Methods in Heat Fluid Flow 21 (1) pp. 61–72.

[17] Magyari, E., Keller, B. (1999). Heat and mass transfer in the boundary layers on an exponentially stretching continuous surface. Journal of Applied Mechanics and Physics 32, pp. 577–85

[18] Makinde, O.D., Aziz, A. (2011). Boundary layer flow of a nanofluid past a stretching sheet with a convective boundary condition. International Journal of Thermal Science 50, pp. 1326–1332.

[19] Miklavcic, M. Wang, C.Y. (2006). Viscous flow due to a shrinking sheet. Applied Mathematics 64, pp. 283–290.

[20] Nield, D.A., Kuznetsov, A.V. (2009). The problem for natural convective boundary layer flow in a porous medium saturated by a noanofluid. International Journal of Heat Mass Transfer 52, pp. 5792–5795.

[21] Samir, K.N., Pop, I. (2014). Effects of magnetic field and thermal radiation on stagnation flow and heat transfer of nanofluid over a shrinking surface, International Communication in Heat and mass transfer 53, pp. 50-55.

[22] Wang, C.Y. (2008). Stagnation flow towards a shrinking sheet. International Journal of Nonlinear Mechanics 43, pp. 377–382.